

Simplified Modelling of Heat Transfer in Groundwater

Jerzy M. Sawicki

Faculty of Hydro and Environmental Engineering, Technical University of Gdańsk
ul. Narutowicza 11/12, 80-952 Gdańsk, Poland

(Received April 5, 2001; revised September 25, 2001)

Abstract

The paper deals with a 2D mathematical model, which describes the groundwater temperature. Such a model is an interesting alternative for 3D equations, which require much more additional information (i.e. shape and characteristics of the area, initial and boundary conditions) than 2D equations. In the first part of the paper the equations of energy conservation for two main versions of a 2D model (i.e. for a confined and for an unconfined area) were derived. Special attention was paid to two kinds of heat-transfer processes, viz. micro-dispersion, caused by pore-space averaging of the temperature and velocity, and macro-dispersion, due to averaging along the water-layer depth. The analysis of the thermal conditions in the region of the Koziernice electric-power-plant was presented, as an example of the model application.

Notation

The following symbols are used in this paper:

- a – auxiliary function,
- A_b, A_f – auxiliary function,
- b – auxiliary function,
- c – concentration of dissolved matter,
- c^o – deviation of concentration,
- c_f – specific heat of a fluid,
- C_1, C_2 – integration constants,
- d_p – mean diameter of ground particles,
- D_M – coefficient of molecular diffusion (scalar),
- D_T – coefficient of thermal molecular diffusivity (scalar),
- e_{Tb}, e_{Tf} – effective unit heat energy fluxes, through the bottom (b) and free-surface (f),

\mathbf{E}_T	- coefficient of effective heat dispersion (tensor for anisotropic case),
E_T	- coefficient of effective heat dispersion (scalar for isotropic case),
f	- optional function,
F	- auxiliary function,
g	- gravity acceleration,
G_T	- thermal diffusivity of ground,
h_c	- coefficient of heat exchange between water and porous medium,
H	- water layer depth,
i_b, i_f	- bottom slope and free-surface slope,
I_m	- number of functions s_{mi} ,
I_T	- number of functions s_{Ti} ,
\mathbf{K}	- hydraulic conductivity (tensor for anisotropic case),
K	- hydraulic conductivity (scalar for isotropic case),
K_D	- coefficient of dissolved matter macro-dispersion (scalar for isotropic case),
\mathbf{K}_E	- coefficient of total heat dispersion in porous medium (tensor for anisotropic case),
K_E	- coefficient of total heat dispersion in porous medium (scalar for isotropic case),
\mathbf{K}_M	- coefficient of dissolved matter micro-dispersion (tensor for anisotropic case),
K_M	- coefficient of dissolved matter micro-dispersion (scalar for isotropic case),
\mathbf{K}_T	- coefficient of heat micro-dispersion (tensor for anisotropic case),
K_T	- coefficient of heat micro-dispersion (scalar for isotropic case),
n_e	- effective porosity,
\mathbf{n}_g	- unit vector, normal to the considered surface,
p	- pressure,
p_o	- reference pressure (e.g. $p_o = p_{atm} =$ atmospheric pressure),
P	- pressure function,
Pe	- Peclet number,
\mathbf{q}	- Darcy flux (specific discharge),
\mathbf{q}_D	- macro-dispersive unit flux of thermal energy,

- q_E – total unit flux of thermal energy,
 q_H – micro-dispersive unit flux of thermal energy,
 q_M – molecular unit flux of thermal energy,
 q_T – effective unit flux of thermal energy,
 Q – discharge of water,
 r – radius,
 Re – Reynolds number,
 s_{mi} – mass source function,
 s_{Ti} – thermal energy source function,
 S_s – storage coefficient (storativity for confined aquifers, specific yield for unconfined aquifers),
 t – time,
 T – pore-space averaged temperature,
 T^x – deviation of the real temperature ($T^x = T_r - T$),
 T^o – deviation of the depth-averaged temperature ($T^o = T - \theta$),
 T_r – real temperature of the groundwater,
 T_s – temperature of the porous medium,
 u – real velocity of the groundwater,
 u^x – deviation of the real velocity ($u^x = u - u_p$),
 u_p – pore velocity (“heat-front-velocity”),
 v – depth-averaged velocity of the groundwater,
 v^o – deviation of the pore velocity ($v^o = u_p - v$),
 w – effective influent of water to the aquifer,
 x, y – horizontal Cartesian co-ordinates,
 z – vertical Cartesian co-ordinates,
 z_b – aquifer floor ordinate,
 z_f – aquifer roof ordinate (for confined flows) or free-surface ordinate (for unconfined flows),
 β_x, β_y – angles between the axes Ox, Oy and free-surface element ΔS_r ,
 δ – Kronecker delta,
 ΔE_{Tf} – elementary flux of heat energy through the element ΔS_r ,
 ΔS – projection of ΔS_r on the xOy -plane,
 ΔS_r – element of the free-surface,
 θ – depth-averaged groundwater temperature,
 θ_s – depth-averaged porous medium temperature,

- λ – groundwater thermal conductivity,
- λ_g – porous medium thermal conductivity,
- ν – kinematic viscosity of water,
- ρ – fluid density,
- ρ_o – fluid density for $p = p_0$,
- φ – filtration potential.

attention: the bar denotes depth-averaged value.

1. Introduction

The heat energy does not belong to those factors, which are always very harmful for the quality of groundwater, like heavy metals compounds, organic pollutants or micro-organisms. However, in ecological practice one has very often to solve problems connected with the description of the groundwater temperature. Such problems appear during investigations of hydrogeological conditions in the neighbourhood of electric-power-plants, heat-generating plants, energetic pipelines or when frost penetration into the ground is considered.

In general, the field of the groundwater temperature changes in space and time, so must be described by means of 3D-equations. However, spatial models are time-consuming and expensive, as in order to exploit such a tool one has to formulate 3D initial conditions and 3D data for the model verification. To deliver such information, very precise control bore-holes must be performed and sets of multiple piezometers (i.e. with filters at different depths) must be installed in the region considered.

For many problems simplified 2D horizontal models of heat exchange are sufficient. Such models can be applied only in those cases where the flow is exactly two-dimensional, or when vertical flow components can be neglected. However, these restrictions are not very serious in many cases, so a 2D model is an important tool for tackling hydrogeological problems.

2. Equations for 3D Cases

The groundwater velocity field, in the saturation zone, can generally be described by the filtration potential (piezometric head), which is expressed as a solution of the Richards equation (Verruijt 1970, Zaradny 1990):

$$\rho_o S_s \frac{\partial \varphi}{\partial t} = \operatorname{div} (\rho \mathbf{K} \operatorname{grad} \varphi) + \sum_{i=1}^{I_m} S_{mi} \quad (1)$$

where for incompressible fluids:

$$\varphi = z + p/\rho g \quad (2)$$

and for compressible fluids:

$$\varphi = z + P/g = z + \int_{p_0}^p dp/(\rho g) \quad (3)$$

where φ – filtration potential, ρ – fluid density, S_S – storage coefficient, t – time, \mathbf{K} – tensor of hydraulic conductivity, z – vertical ordinate, p – pressure, p_0 – reference pressure, $\rho_0 = \rho$ for $p = p_0$, g – gravity acceleration, s_{mi} – source function, I_m – number of source functions, P – pressure function. The velocity field can be determined by means of the Darcy law:

$$\mathbf{q} = -\mathbf{K} \text{grad } \varphi \quad (4)$$

(\mathbf{q} – Darcy flux). For isotropic aquifers the hydraulic conductivity is a scalar value (K).

The temperature of groundwater is described by the energy conservation equation. In a general case, taking into account different physical properties of a fluid and a porous medium, we have to write a separate equation for the heat transfer in the fluid (Dagan 1972):

$$\frac{\partial T}{\partial t} + \text{div}(\mathbf{u}_p T) = \text{div}(\mathbf{E}_T \text{grad } T) + h_c (T_S - T) + \sum_{i=1}^{I_T} s_{Ti} \quad (5)$$

and separately for the porous medium:

$$\frac{\partial T_S}{\partial t} = G_T \Delta T_S + h_c (T - T_S) \quad (6)$$

where: T – fluid temperature, averaged in pore-space, T_S – porous medium temperature, \mathbf{u}_p – pore velocity, \mathbf{E}_T – tensor of effective heat dispersivity, h_c – coefficient of heat exchange between fluid and porous medium, s_{Ti} – temperature source function, I_T – number of temperature source functions, G_T – heat diffusivity of the porous medium. For the slow flows, when the Reynolds number (Re) meets the condition:

$$Re = u_p d_p / \nu \leq 1 \quad (7)$$

(d_p – mean diameter of ground particles, ν – the fluid kinematic viscosity), the difference between the processes of heat transfer – in the fluid and through the porous medium – becomes negligible. In such cases we can assume, that $T_S = T$ (Dagan 1972).

The groundwater (or another fluid) can flow through the porous medium in confined areas (artesian filtration) or in unconfined areas. In the first case the shape of the aquifer is defined by its geological characteristic. With a more complex situation we have to do considering unconfined flows, when the upper

part of the domain is defined by the free-surface of groundwater. The shape of this surface is described by the following kinematic condition (Jin and Kranenburg 1993):

$$\frac{\partial z_f}{\partial t} + u_{px}(z = z_f) \frac{\partial z_f}{\partial x} + u_{py}(z = z_f) \frac{\partial z_f}{\partial y} = u_{pz}(z = z_f) + w \quad (8)$$

where: w – function, which describes changes of the groundwater free-surface, due to the inflow or outflow of water; this function expresses the thickness of the water layer (present in the porous medium), related to the unit of time, which flows in ($w > 0$) or out ($w < 0$) from the aquifer.

In a general case, the shape of the aquifer floor can also vary in space and time. Its ordinate is described by the kinematic condition on the aquifer bottom:

$$\frac{\partial z_b}{\partial t} + u_{px}(z = z_b) \frac{\partial z_b}{\partial x} + u_{py}(z = z_b) \frac{\partial z_b}{\partial y} = u_{pz}(z = z_b). \quad (9)$$

3. Equations for 2D Unconfined Flows

If the vertical components of the pore velocity vector \mathbf{u}_p do not exert any important influence on the course of considered phenomena, we can make use of a simplified model of the flow. In this model the flow variables are averaged with respect to the vertical ordinate.

The free-surface level in such a case is described by the classic Boussinesq equation (Verruijt 1970, Zaradny 1990), which has the following form for unconfined flow:

$$\bar{n}_e \frac{\partial z_f}{\partial t} = \text{div}(\mathbf{K} H \text{grad} z_f) + w \cdot \bar{n}_e. \quad (10)$$

For the confined flow this equation has the shape:

$$\bar{S}_s H \frac{\partial \bar{\varphi}}{\partial t} = \text{div}(\mathbf{K} H \text{grad} \bar{\varphi}) \quad (11)$$

where the bar denotes depth-averaged values.

After determination of z_f (or $\bar{\varphi}$ respectively) we can calculate the depth-averaged Darcy flux \mathbf{q} (or depth-averaged pore velocity \mathbf{v}), making use of the averaged Darcy law (Eq. 4):

$$\mathbf{q} = \bar{n}_e \mathbf{v} = -\mathbf{K} \text{grad} z_f \quad (\text{unconfined flow}), \quad (12)$$

$$\mathbf{q} = \bar{n}_e \mathbf{v} = -\mathbf{K} \text{grad} \bar{\varphi} \quad (\text{confined flow}). \quad (13)$$

In order to describe the mean temperature distribution we have to average the equation of energy conservation (Eq. 5). Real temperature T in the model considered must be presented as the sum of the depth-averaged temperature θ and the temperature deviation T° :

$$T(x, y, z, t) = \theta(x, y, t) + T^\circ(x, y, z, t). \quad (14)$$

Integrating both sides of Eq. 5 with respect to the vertical variable, substituting the kinematic conditions (Eqs. 8, 9) and also substituting the Boussinesq equation, we obtain:

$$\frac{D\theta}{Dt} = -\frac{1}{H} \left[\operatorname{div} \left(\frac{1}{\rho c_f} \mathbf{q}_T H + H \overline{\mathbf{v}^\circ T^\circ} \right) \right] + \frac{1}{H} (e_{Tf} + e_{Tb}) + \bar{h}_c (\theta_s - \theta) + \sum_{i=1}^{I_T} \bar{s}_{Ti}. \quad (15)$$

Carrying out the analogic transformations for Eq. 6, we can write:

$$\frac{\partial \theta_s}{\partial t} = G_T \Delta \theta_s + \bar{h}_c (\theta - \theta_s). \quad (16)$$

Relations (15, 16), together with the Boussinesq equation (Eq. 10) and Darcy law (Eq. 12) establish the system of mathematical equations, closed with respect to unknowns θ , θ_s , z_f and \mathbf{q} , which describe the 2D heat transfer in an unconfined aquifer.

4. Equations for 2D Confined Flows

The scheme of a confined aquifer is shown in Fig. 1b. The equation of energy conservation for such a case can be obtained in almost the same way as for an unconfined aquifer. A slight difference appears when we want to pose the problem. In the case of an unconfined aquifer, the functions $H(x, y, t)$ and $\mathbf{v}(x, y, t)$ can be calculated after determination of $z_f(x, y, t)$ from the Boussinesq equation (10), whereas for the confined aquifer the function $H(x, y, t)$ is known from the very beginning, as it belongs to the geological characteristics of the situation considered. The mean velocity \mathbf{v} is defined by Eq. 13, when we know the solution of Eq. 11.

5. Micro- and Macro-dispersion of Heat Energy

Appearing in the Eq. 15 symbol \mathbf{q}_T denotes the depth-averaged relative unit flux of heat energy, encompassing global effects of the molecular heat conduction and so-called hydrodynamic dispersion (Rumer 1972):

$$\mathbf{q}_T = \mathbf{q}_M + \mathbf{q}_H = -\rho c_f [D_T \cdot \operatorname{grad} T + \overline{T^x \mathbf{u}^x}], \quad (17)$$

$$T^x = T_r - T, \quad \mathbf{u}^x = \mathbf{u} - \mathbf{u}_p \quad (18)$$

where: D_T – thermal diffusivity of a fluid, T_r – real temperature of groundwater, \mathbf{u} – real velocity of groundwater.

According to the commonly applied practice (Rumer 1972), the term describing hydrodynamic dispersion is expressed by the generalised Fourier law. Adding

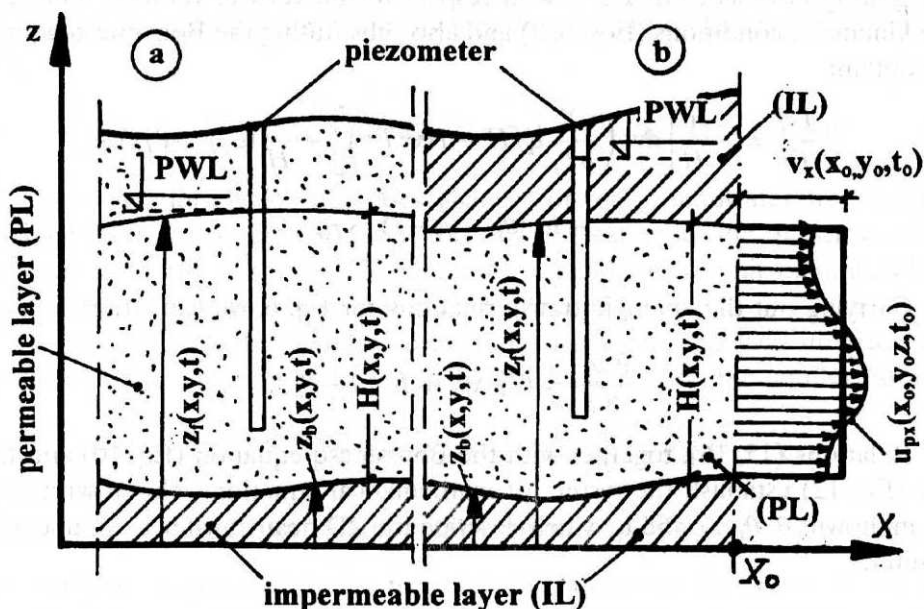


Fig. 1. Co-ordinate system and calculation schemes for confined (a) and unconfined (b) flows (PWL = piezometric water level)

influences of both unit processes (i.e. molecular conduction and hydrodynamic dispersion) we can define the effective unit flux of heat energy as:

$$\begin{aligned} q_T &= -\rho c_f [D_T \text{grad } T + K_T \text{grad } T] = -(D_T + K_T) \rho c_f \text{grad } T = \\ &= -\rho c_f E_T \text{grad } T. \end{aligned} \quad (19)$$

The coefficient D_T is a material constant. For the process of unsteady heat conduction in the groundwater it is assumed, that (Dagan 1972):

$$D_T = 2\lambda / (3\rho c_f), \quad D_T = D_T \cdot \delta \quad (20)$$

(λ – thermal conductivity for pure water, c_f – specific heat of water). For the steady state we have:

$$D_T = [n_e \lambda + (1 - n_e) \lambda_g] / [\rho c_f n_e + \rho_g c_g (1 - n_e)] \quad (21)$$

where c_g – specific heat of the ground.

The coefficient K_T in turn depends on the flow character. For the Peclet numbers:

$$Pe = \frac{v d_p}{D_T} \leq 10\,000 \quad (22)$$

its value is equal to the coefficient of mass dispersion K_M . For the isotropic ground one can assume (Dagan 1972):

$$K_T = 1.4 v d_p, \quad K_T = K_T \cdot \delta. \quad (23)$$

For the anisotropic media one has to determine two values, viz. longitudinal and transversal components of heat dispersion, e.g. making use of the theory of dissolved matter dispersion (Fischer 1979, Rutherford 1994), and subsequently transforming these components into the optional co-ordinate system (Sawicki 1994). When the Peclet number $Pe < 3000$, one can neglect heat dispersion in comparison with the heat conduction, assuming in this case that $K_T = 0$ (Dagan 1972).

Let us note, that in Eq. 15 the depth-averaged value of the vector \mathbf{q}_T appears, and alongside this vector there is an expression \mathbf{q}_D , where:

$$\mathbf{q}_D = -\overline{T^o \mathbf{v}^o}. \quad (24)$$

This function is analogical with the vector \mathbf{q}_H . The difference lies in the character of components of these expressions - \mathbf{q}_H is defined by deviations of velocity and temperature in the pore space (\mathbf{u}^X and T^X), whereas \mathbf{q}_D is a depth-averaged product of "macro-deviations" (\mathbf{v}^o and T^o), determined along the vertical ordinate "z". Taking into account this difference, it is very profitable to distinguish two kinds of dispersive unit fluxes of heat energy, namely a micro-dispersive unit heat flux (\mathbf{q}_H) and a macro-dispersive unit heat flux (\mathbf{q}_D).

Methods of the vector \mathbf{q}_D description have not been developed so far. An analogical vector, describing the macro-dispersion of dissolved matter, was investigated by Sawicki (1995). An analysis of the process pointed to the conclusion, that the unit flux of mass, due to the macro-dispersion, can be expressed by the following generalisation of Fick's law:

$$\overline{c^o \mathbf{v}^o} = -K_D \text{grad } \bar{c} = 6.85 (i_b - i_f)^2 K_M \text{grad } \bar{c} \quad (25)$$

(K_D - coefficient of dissolved matter macro-dispersion, $i_b = |\text{grad } z_b|$ - aquifer roof slope, $i_f = |\text{grad } z_f|$ - aquifer floor slope, c - depth-averaged concentration).

As long as the problem of heat energy macro-dispersion is completely solved, one can make use of a provisional definition of the coefficient K_E (Sawicki 1995):

$$K_E = D_T + 1.4 \nu d_p \left[1 + 6.85 (i_b - i_f)^2 \right] \quad (26)$$

for the total unit mass flux ($\mathbf{K}_E = K_E \cdot \delta$, for the isotropic case):

$$\mathbf{q}_E = \bar{q}_M + \mathbf{q}_H + \mathbf{q}_D = -\mathbf{K}_E \text{grad } \theta. \quad (27)$$

When $i_b = i_f$, the vertical velocity profile is uniform, macro-dispersion does not occur and we have to do only with a combination of diffusion and micro-dispersion ($K_E = D_T + K_T$).

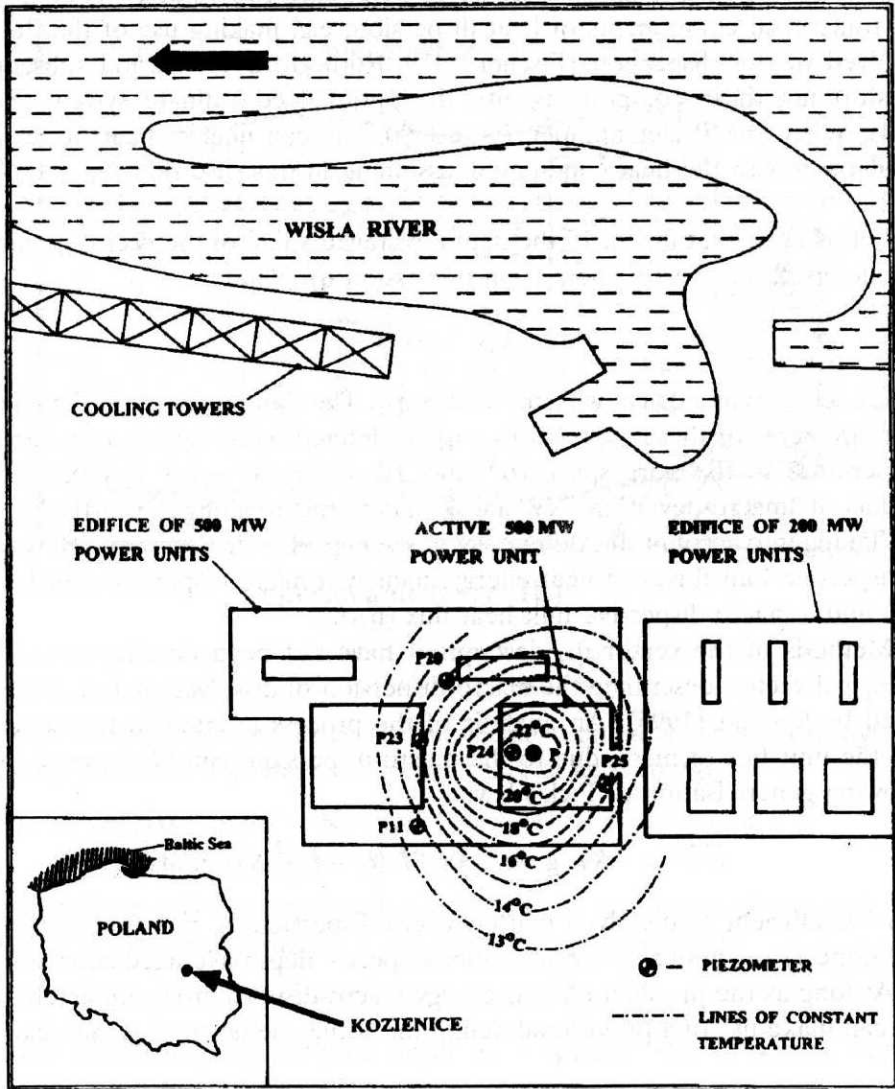


Fig. 2. Position of the power-plant edifices and measured groundwater temperature

6. Example of the Model Application

6.1. Characteristics of the Situation

The active power unit 500 MW of the Koziencice-power-plant (Fig. 2) is under special control, because of the low load capacity of the subsoil. Monitoring of hydrogeological parameters in observation wells in this unit neighbourhood

(piezometers P11, P20, P23, P24, P25), led to the conclusion that the groundwater temperature near the power boiler is apparently heightened. The system of constant-temperature lines, shown in Fig. 2, was drawn on the base of measurements carried out in 1993–1996 by the technical services of the power-plant. The set of data was delivered together with the remaining initial pieces of information. For this reason it was not possible to discuss these data nor to change them, as the ordered scope of investigations did not include any measurements.

Explanation of the temperature rise reasons was very important for the power-plant managers. Especially important was indication of the main cause of the observed situation – was the temperature growth caused by the heat conduction only, or mainly by the possible outflow of hot water from leaks in the power-unit installations?

As can be seen in Fig. 2, the set of constant-temperature lines around the power-unit is regular, almost symmetric. The centre of symmetry (point P in Fig. 2) is situated under the active power-unit. This symmetry enables us to exclude a single-directional outflow of the heated groundwater from possible reasons of temperature growth, as in the other case we would observe “a tongue” of hot water, oriented towards the outflow. This conclusion is confirmed by the groundwater table ordinates observed in piezometers and delivered by the power-plant technical service. These ordinates are almost constant and equal to 100.9 m a.s.l. (Fig. 3), as under the power-plant edifices there is the flat part of the groundwater table, depressed by dewatering systems (drains and wells).

However, the axisymmetric shape of the system of constant-temperature lines does not exclude a possible leak of hot water; flowing uniformly in all horizontal directions. Such a leak would not exert any important influence on the free-surface shape, but would influence the temperature field. Trying of this question is the main purpose of the work presented in this example.

The problem was solved in two ways, according to the main question, posed by the orderer (i.e. the Koziernice power-plant authorities). In the first attitude it was assumed, that the leak did not exist ($v = 0$) and then the measured temperature distribution was compared with the distribution obtained as a solution of the equation of pure heat conduction (problem TI).

In the second step it was assumed that the leak in point P (see Fig. 2) existed and the system of measured constant-temperature lines was compared with that obtained from the equation of heat advection–conduction (problem TII).

6.2. The TI Problem – Pure Heat Conduction

The calculation scheme for the problem of heat transfer by pure conduction is shown in Fig. 3a. The ground parameters in the neighbourhood of the power-plant are very uniform (alluvial sand), hence it was assumed, that the aquifer under the power-unit is isotropic (hydraulic conductivity $K = 0.00028$ m/s, effective

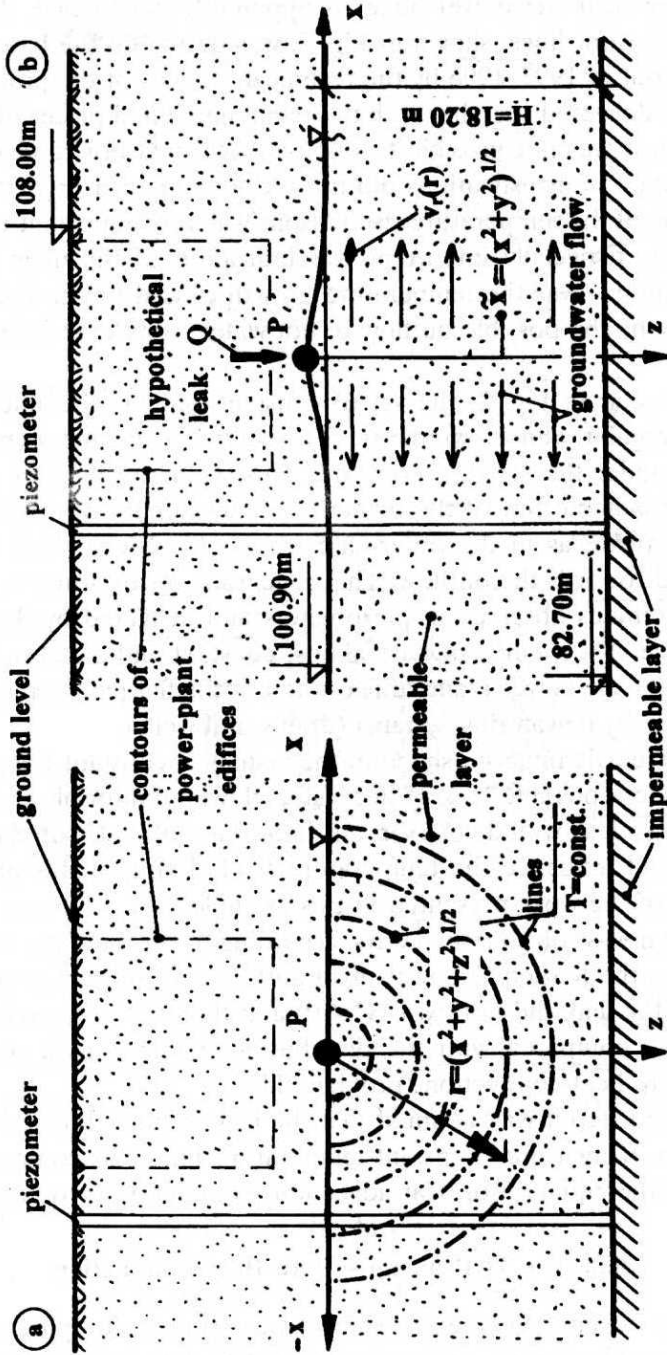


Fig. 3. Calculation schemes for pure conduction (a) and for advection-conduction (b)

porosity $n_e = 0.35$, water thermal conductivity $\lambda = 0.534 \text{ J/msr}^\circ\text{C}$, air thermal conductivity $\lambda_a = 0.0308 \text{ J/msr}^\circ\text{C}$, ground thermal conductivity $\lambda_g = 1.000 \text{ J/msr}^\circ\text{C}$, water specific heat $c_f = 4181 \text{ J/kg}^\circ\text{C}$, ground specific heat $c_g = 830 \text{ J/kg}^\circ\text{C}$. Effective thermal conductivity of the saturation zone ($0.8369 \text{ J/ms}^\circ\text{C}$) and of the aeration zone ($0.6608 \text{ J/ms}^\circ\text{C}$) are quite close, so for the technical approximation one can consider the spatial heat transfer, around the point P (Fig. 3a), when the solution $T(r)$ depends only on the radius r . For the steady-state conditions one can rewrite the Eq. 5 as follows (spherical co-ordinates – Fig. 3a):

$$\frac{d}{dr} \left(r^2 \frac{dT}{dr} \right) = 0. \quad (28)$$

This relation can be easily integrated, which yields:

$$T(r) = -C_1/r + C_2. \quad (29)$$

The obtained function describes the theoretical distribution of the temperature in the half-space under the considered power-unit (with the centre at point P). Taking into account the length of piezometers and mixing of water in observation wells during measurements, we must consider the measured temperature as depth-averaged values (θ). In this situation we have to average the Eq. 46 with respect to the vertical variable “z”, which yields:

$$\begin{aligned} \theta(\tilde{x}) &= \frac{1}{H} \int_0^H T \left(r = \sqrt{x^2 + y^2 + z^2} \right) dz = \\ &= \frac{1}{H} \int_0^H \left(C_2 - C_1 / \sqrt{x^2 + y^2 + z^2} \right) dz = \\ &= C_2 - C_1 \ln \left| H / \tilde{x} + \sqrt{1 + H^2 / \tilde{x}^2} \right| / H \end{aligned} \quad (30)$$

(the ordinate \tilde{x} must be oriented along the groundwater table, $\tilde{x}^2 = x^2 + y^2$).

Two integration constants C_1 and C_2 one can calculate making use of measured temperatures. We have at our disposal four piezometers (as the distances of P20 and P23 from the point P are equal):

$$\begin{aligned} \tilde{x}_{24} &= 10.0 \text{ m}, & \theta_{24} &= 26.4^\circ\text{C} & \text{for P24} \\ \tilde{x}_{25} &= 42.5 \text{ m}, & \theta_{25} &= 16.9^\circ\text{C} & \text{for P25} \\ \tilde{x}_{20} &= 60.0 \text{ m}, & \theta_{20} &= 15.6^\circ\text{C} & \text{for P20} \\ \tilde{x}_{11} &= 70.0 \text{ m}, & \theta_{11} &= 14.8^\circ\text{C} & \text{for P11} \end{aligned}$$

The integration constant C_2 could be easily calculated, using the evident condition (see Fig. 2), that very far from the edifice the groundwater temperature tends to some constant value (about 12°C in this case). But more difficult is the determination of the second integration constant, namely C_1 . One could suggest

the method of empirical identification of this value, using for example, the least square method. However in this case the theoretical temperature profile would (from definition) show very good conformity with the experimental data, whereas the purpose of this investigation was to determine the reason for temperature rise.

In this situation an atypical (but logical) attitude was applied. Namely, for each two temperatures the values of C_1 and C_2 were computed, whereas two remaining temperatures served for model verification. Effectively we have 6 possible combinations of the function (30):

$C_1 = -182.7$ [$m^\circ C$],	$C_2 = 12.7$ [$^\circ C$]	for TI-A (P24, P25)
$C_1 = -183.1$ [$m^\circ C$],	$C_2 = 12.6$ [$^\circ C$]	for TI-B (P24, P20)
$C_1 = -190.2$ [$m^\circ C$],	$C_2 = 12.1$ [$^\circ C$]	for TI-C (P24, P11)
$C_1 = -185.7$ [$m^\circ C$],	$C_2 = 12.6$ [$^\circ C$]	for TI-D (P25, P20)
$C_1 = -239.3$ [$m^\circ C$],	$C_2 = 11.5$ [$^\circ C$]	for TI-E (P25, P11)
$C_1 = -400.0$ [$m^\circ C$],	$C_2 = 9.2$ [$^\circ C$]	for TI-F (P20, P11)

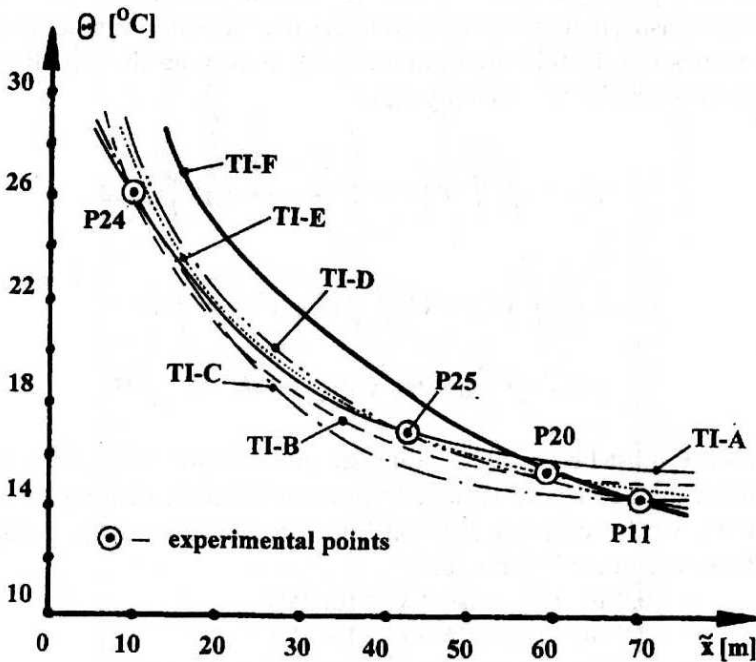


Fig. 4. Temperature distribution for case TI

The diagrams of these versions of the function (30) are shown in Fig. 4. The shape of these curves confirms the hypothesis that the temperature rise in the region of the power-unit is caused by pure heat convection (see discussion below).

6.3. Problem TII – Advection and Conduction

For the second model of the problem under consideration it was assumed that the hypothetical leak of discharge Q in the power boiler installation and/or construction, causes an axisymmetrical spreading of the hot water (Fig. 3b). Taking into account, that in this case $i_b = i_f = 0$ and $\delta/\delta t \equiv 0$, we can write the following version of Eq. 15 (in polar coordinates, assuming the axial symmetry):

$$v_r \frac{\partial \theta}{\partial r} = \frac{1}{r} \frac{\partial}{\partial r} \left[(D_T + 1.4v_r d_p) r \frac{\partial \theta}{\partial r} \right]. \quad (31)$$

The depth-averaged flow velocity v_r can be expressed by the flow discharge Q :

$$v_r(r) = Q / (2\pi Hr). \quad (32)$$

According to Eq. 21, the thermal diffusivity is equal to:

$$D_T = (0.35 * 0.534 + 0.65 * 1.00) / (4181.0 * 1000.0 * 0.35 + 830.0 * 2700 * 0.65) = 0.286 * 10^{-6} \text{ [m}^2/\text{s}] \quad (33)$$

Assuming even unrealistic discharge of leaking water $Q = 0.1 \text{ [m}^3/\text{s]}$ (unrealistic, because such discharge would be recorded by the power-plant control system), we would have in the piezometer P24 ($r_{24} = 10.0 \text{ m}$) velocity $v_r = 8.7 * 10^{-5} \text{ [m/s]}$, so for alluvial sands ($d_p = 0.0005 \text{ m}$) we could write:

$$K_T = 1.4v_r d_p = 0.06 * 10^{-6} \text{ [m}^2/\text{s}] < D_T = 0.286 * 10^{-6} \text{ [m}^2/\text{s}] \quad (34)$$

This evaluation means that in comparison with heat conduction we can neglect heat dispersion (as in this case $Pe = 0.3 < 3000$), and write a simplified form of the Eq. 31:

$$v_r \frac{\partial \theta}{\partial r} = \frac{D_T}{r} \frac{\partial}{\partial r} \left(r \frac{\partial \theta}{\partial r} \right). \quad (35)$$

The latter equation has the following analytical solution (which can be proved substituting Eq. 36 into Eq. 35):

$$\theta(r) = C_1 r^F / F + C_2 \quad (36)$$

where:

$$F = Q / (2\pi H D_T). \quad (37)$$

Eq. 36 is not valid for $Q = 0$ (see Bronsztejn 1968). For this special case we have a different solution of the Eq. 35, namely:

$$\theta^0(r) = C_1 \ln(r/C_2). \quad (38)$$

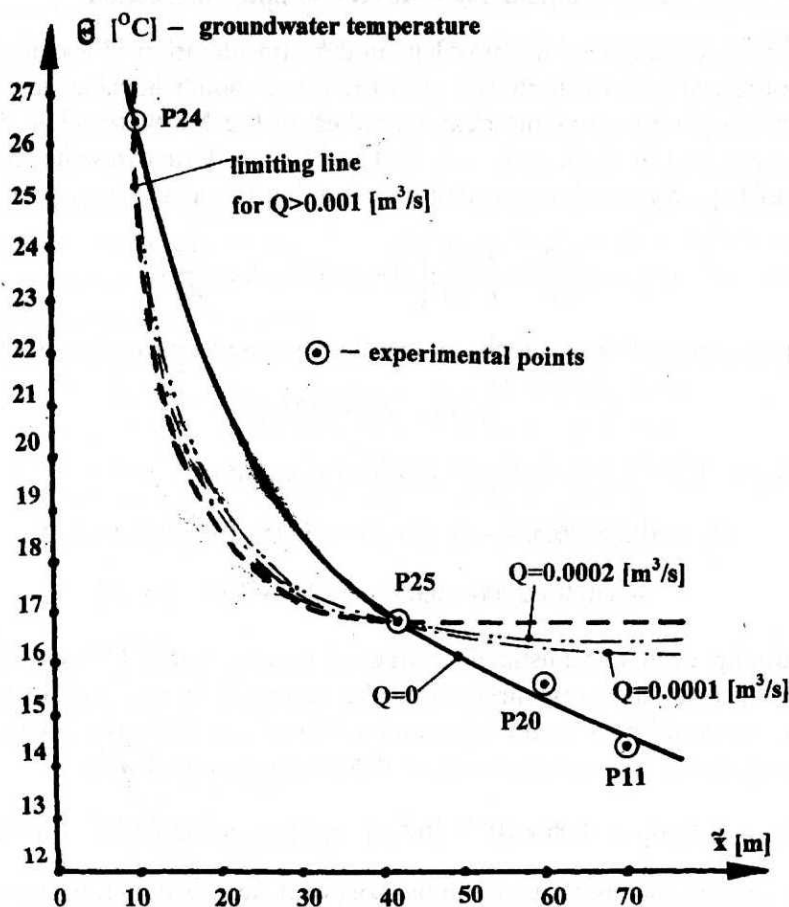


Fig. 5. Temperature distribution case III

We can determine integration constants as in the first problem (TI), making use of experimental data. Analysis of the obtained results leads to the conclusion that together with the increase of function "F" and distance "r", the temperature θ tends to the constant value (where $Q > 0.001$ [m^3/s]). For the case shown in Fig. 5, constants $C_1 = -0.00031$ ($^{\circ}\text{C m}^{-3.1}$), as for this case $F = 3.1$, and $C_2 = 26.5^{\circ}\text{C}$ were calculated for temperatures θ_{24} and θ_{25} , and then the shape of the line $\theta(r)$ was analysed for different water discharges Q (which are equivalent to different velocities of groundwater). It turned out that this line tends towards experimental values of temperature θ_{20} and θ_{11} when $Q \rightarrow 0$, which means that the best coincidence between experimental data and theoretical prediction in this case (TII) we obtain for pure conduction ($v = 0$).

The rise of the groundwater temperature analysed in this paper, causes some additional heat energy loss E_L , which can be calculated easily, using the Fourier

law for the first model (for the mean value of the constant $C_1 = -230 \text{ m}^\circ\text{C}$):

$$E_{L1} = -2\pi [\lambda n_e + \lambda_g(1 - n_e)] C_1 = 1.21 \text{ kW} \quad (39)$$

and for the second model (the advective energy flux only, as the thermal conduction can be neglected in this case), for $Q = 0.0001 \text{ m}^3/\text{s}$:

$$E_{L2} = Qc_f\rho C_2 = 11.08 \text{ kW} \quad (40)$$

In comparison with the total energy production of the power-plant (500 MW for the unit considered), both energy losses are negligible, although in the second case the value of 11 kW could play some role in the total financial balance. Fortunately, the temperature rise is apparently caused only by the unavoidable heat conduction.

7. Conclusions

As can be seen in Fig. 4, all curves $\theta(r)$ are located close together, forming a band $(2-4)^\circ\text{C}$ wide. These curves, from the technical point of view, show a quite acceptable coincidence with the system of experimental points. The worse concurrence is for lines determined using the temperature θ_{11} , measured in the piezometer P11, the most distant from the heat source (point P). One cannot exclude, that this piezometer is situated in the zone of more apparent groundwater flow, due to the drainage system functioning. However, even in this point the discrepancy is negligible. Finally, taking into account results of the task TII, one can state that the temperature growth in the neighbourhood of the power unit 500 MW is caused only by pure heat conduction between the power boiler and the foundation and ground.

As far as the mathematical equations of the heat transfer are concerned, one can also say that the 2D model, derived and discussed in this paper, is a very useful and convenient tool for the solving of practical problems.

Acknowledgements

The author would very much like to thank the Authorities of the Kozenice power-plant for their financial support and for experimental data, which made possible completing of the work, presented in this paper.

References

- Bear J., Bachmat Y. (1990), *Introduction to modelling of transport phenomena in porous media*, Kluwer Academic Publishers, London.
- Bronsztejn I. N., Siemiendajew K. A. (1968), *Matematyka. Poradnik encyklopedyczny*, PWN, Warszawa.

- Dagan G. (1972), *Some aspects of heat and mass transfer in porous media*, in: *Fundamentals of transport phenomena in porous media*, Development in Soil Science 2. IAHR. Elsevier Publ.Comp., Amsterdam-London-New York.
- Fischer H. B. et al. (1979), *Mixing in inland and coastal waters*, Academic Press, New York.
- Jin X. and Kranenburg C. (1993), Quasi-3D numerical modelling of shallow water circulation, *J. of Hydr. Eng.*, 119(4).
- Nassar I. N., Horton R. (1992), Simultaneous transfer of heat, water and solute in porous media, *Soil Sci. Soc. Am. J.*, Vol. 56.
- Rumer R. R. (1972), On the derivation of a convective-dispersion equation by spatial averaging, in: *Fundamentals of transport phenomena in porous media*, *Development in Soil Science 2. IAHR*, Elsevier Publ. Comp., Amsterdam-London-New York.
- Rutherford J. C. (1994), *River mixing*, John Wiley and Sons, Chichester.
- Sawicki J. M. (1994), *Plane dispersion of pollutants*, in: *Hydrological, Chemical and Biological Processes of Transformation and Transport of Contaminants in Aquatic Environment*, IAHS Publication No. 219.
- Sawicki J. M. (1995), One-dimensional macro-dispersion in confined aquifers, *Proceedings of HYDRA-2000*, Vol. 4, Thomas Telford, London.
- Verruijt A. (1970), *Theory of groundwater flow*, Macmillan and Co., Delft.
- Zaradny H. (1990), *Matematyczne metody opisu i rozwiązań zagadnień przepływu wody w nienasyconych i nasyconych gruntach i glebach*, Prace IBW PAN, Nr 23.